Radio-Frequency Spectroscopy of Ultracold Fermions

S. Gupta[1], Z. Hadzibabic[1], M.W. Zwierlein[1], C.A. Stan[1], K. Dieckmann[1], C.H. Schunck[1], E.G.M. van Kempen[2], B.J. Verhaar[2] and W. Ketterle[1]

[1] *Department of Physics, MIT-Harvard Center for Ultracold Atoms, and Research Laboratory of Electronics, MIT, Cambridge, MA 02139*

[2] *Eindhoven University of Technology, P.O. Box 513, 5600 MB Eindhoven, The Netherlands*

Radio-frequency techniques were used to study ultracold fermions. We observed the absence of mean-field "clock" shifts, the dominant source of systematic error in current atomic clocks based on bosonic atoms. This is a direct consequence of fermionic antisymmetry. Resonance shifts proportional to interaction strengths were observed in a three-level system. However, in the strongly interacting regime, these shifts became very small, reflecting the quantum unitarity limit and many-body effects. This insight into an interacting Fermi gas is relevant for the quest to observe superfluidity in this system.

arXiv:cond-mat/0307259v1 [cond-mat.soft] 10 Jul 2003

Radio-frequency (RF) spectroscopy of ultracold atoms provides the standard of time. However, the resonance frequencies are sensitive to the interactions between atoms, leading to the so-called clock shifts of the unperturbed resonances [1]. These shifts limit the accuracy of current atomic clocks [2,3], but can also be used to characterize atomic interactions.

RF spectroscopy has previously been applied to cold atoms to determine the size and temperature of atom clouds [4,5]. RF methods have also been used for evaporative cooling, for preparing spinor Bose-Einstein condensates (BEC) [6,7], and as an output coupler for atom lasers [5,8]. In all these experiments, shifts and broadenings due to atomic interactions were negligible. Recently, density-dependent frequency shifts of RF transitions were observed in rubidium [9] and sodium [10] BECs. These frequency shifts are proportional to the difference in mean-field energies of two internal atomic states and allow scattering lengths to be extracted. Mean field shifts in BECs have been observed also by optical spectroscopy [11,12].

Here, we apply RF spectroscopy to ultracold clouds of fermions and demonstrate several phenomena: (1) the absence of a clock shift in a two-level system due to fermionic antisymmetry, (2) the emergence of mean-field shifts in a three-level system after the relaxation of pair correlations, (3) the limitation of mean-field shifts due to the unitarity limit, and (4) the universality of the interaction energy in a dense cloud, independent of the attractive or repulsive nature of the two-particle interactions.

Research in ultracold fermions has advanced rapidly, with six groups now having reached quantum degeneracy [13–18]. A major goal is to induce strong interactions by tuning magnetic fields to scattering resonances (called Feshbach resonances). Under these conditions, Cooper pairs of fermions may form, leading to superfluidity. This would establish a model system for studying Bardeen-Cooper-Schrieffer (BCS) pairing at densities nine orders of magnitude lower than in previous realizations in ^{3}He and superconductors. We show that RF spectroscopy can be used to characterize interactions between fermions in the regime where superfluidity has been predicted [19,20].

Our experimental technique for preparing ultracold fermions has been considerably improved since our earlier work [17,21]. As the Pauli exclusion principle suppresses elastic collisions between identical fermions at low temperatures and prevents evaporative cooling, we cooled fermionic ^{6}Li sympathetically with bosonic ^{23}Na loaded into the same magnetic trap. In contrast to previous work, we cooled both species in their upper hyperfine states ($^{23}\mathrm{Na}: |F, m_F\rangle = |2, +2\rangle$, $^6\mathrm{Li}: |F, m_F\rangle = |3/2, +3/2\rangle$). This led to a reduction of inelastic loss processes, boosting our final fermion atom numbers by 2 orders of magnitude. We could produce BECs containing up to 10 million sodium atoms in the $|2, +2\rangle$ state by evaporatively cooling pure bosonic samples in the magnetic trap. For a Bose-Fermi mixture, the finite heat capacity of the bosons limited the final lithium temperature after the 30 s evaporation cycle to $\sim 0.3\, T_F$ for 10 million fermions and $\sim T_F$ for 50 million fermions [22], where T_F is the Fermi temperature.

The spin states of ^{6}Li of most interest for superfluid pairing are the two lowest states $|1\rangle$ and $|2\rangle$ ($|1/2, +1/2\rangle$ and $|1/2, -1/2\rangle$ at low field), which are predicted to have an inter-state s-wave Feshbach resonance at $\sim$ 800 G [23,24]. However, both states are high-field seeking at these fields, making them unsuitable for magnetic trapping. We therefore transferred the atoms into an optical trap. For these experiments, 6-8 million $|3/2, +3/2\rangle$ lithium atoms were loaded into the optical trap at $T \sim T_F \sim 35\,\mu$K [25]. The atoms were then transferred to the lowest energy state $|1\rangle$, using an adiabatic frequency sweep around the lithium hyperfine splitting of 228 MHz. DC magnetic fields of up to $\sim$ 900 G were applied, a range encompassing the $|1\rangle - |2\rangle$ Feshbach resonance. Using RF-induced transitions near 80 MHz, we could create mixtures of states $|1\rangle$, $|2\rangle$ and $|3\rangle$ ($|3/2, -3/2\rangle$ at low field), and explore interactions between fermions in these states.

Collisions between atoms cause a shift of their energy, which is usually described by the mean-field effect of all the other atoms on the atom of interest. For example, atoms in state $|2\rangle$ experience an energy shift $\frac{4\pi\hbar^2}{m}n_1 a_{12}$ due to the presence of atoms in state $|1\rangle$. Here $\hbar$ is Planck's constant divided by 2π, m is the mass of the atom, n_1 is the density of $|1\rangle$ atoms and a_{12} is the interstate scattering length. We use the convention that positive scattering length corresponds to a repulsive interaction. Density-dependent shifts of the resonance frequency for the transition connecting two states have been observed in laser-cooled [1] and Bose-condensed clouds [9,10].

In the case of ultracold fermions, only interactions between different internal states are allowed. For a system of density n, let us compare the energy of a gas prepared purely in state $|1\rangle$, to a gas in which one atom is transferred into state $|2\rangle$. The energy difference is $h\nu_{12} + \frac{4\pi\hbar^2}{m}na_{12}$, where ν_{12} is the resonance frequency of the non-interacting system. Similarly, the energy difference between a gas prepared purely in state $|2\rangle$, and a gas in which one atom is transferred into state $|1\rangle$ is $h\nu_{12} - \frac{4\pi\hbar^2}{m}na_{12}$.

However, these energy shifts should not affect the resonance for a coherent transfer out of a pure state. For fermions in the initial pure state, the pair-correlation function vanishes at zero distance due to the antisymmetry of the wavefunction. During any coherent transfer process, the state vectors of all the atoms rotate "in parallel" in Hilbert space, i.e. the superposition of the two spin states has the same relative phase for all atoms. Thus, the atoms remain identical and cannot interact in the s-wave regime. The mean-field energy is thus established only after the coherence of the superposition state is lost and the pair correlations have relaxed, forming a purely statistical mixture of the two states.

It is a consequence of Fermi statistics that spectroscopic methods do not measure the equilibrium energy difference between the initial and final state of the system, but rather the unperturbed resonance frequency. The expected absence of the clock shift has led to suggestions for the use of fermions in future atomic clocks [26]. Our work presents an experimental demonstration of this phenomenon.

We determined the transition frequency between states $|1\rangle$ and $|2\rangle$, first starting with a pure state $|1\rangle$, and then with a pure state $|2\rangle$ sample. The absence of a splitting between these two lines proves the suppression of the clock shift. Fig. 1 shows an example of such measurements. The magnetic field was ramped up to 570 G with the cloud in state $|1\rangle$. At this field, $a_{12} \sim 150\,a_0$. Therefore, the expected equilibrium mean-field shifts were $\Delta\nu = \pm 5$ kHz for our mean density of $3 \times 10^{13}\,\mathrm{cm}^{-3}$ [27]. The interaction between states $|1\rangle$ and $|2\rangle$ at this magnetic field was also observed in the mutual evaporative cooling of the two states in the optical trap. RF pulses of 140 μs duration were applied at frequencies near the unperturbed resonance $\nu_{12} \sim 76$ MHz. Atoms in states $|1\rangle$ and $|2\rangle$ could be monitored separately by absorption imaging, since they are optically resolved at this field. We observed a suppression of the clock shift by a factor of 30 (Fig. 1). Using the same method, the absence of the clock shift was observed at several other magnetic fields. In particular, we observed a suppression of more than three orders of magnitude at ~ 860 G [28].

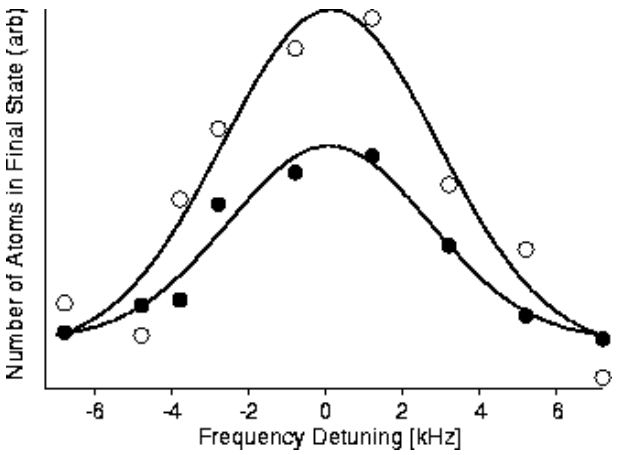

FIG. 1. Absence of the clock shift. RF transitions were driven between states $|1\rangle$ and $|2\rangle$ on a system prepared purely in state $|1\rangle$ (filled circles), and purely in state $|2\rangle$ (open circles). Mean-field interactions would result in 5 kHz shifts for the two curves in opposite directions. Gaussian fits (solid lines) to the data are separated by 0.04 ± 0.35 kHz. This gives a clock shift suppression factor of 30.

P-wave interactions could lead to a non-vanishing clock shift. However, at these low temperatures they are proportional to T or T_F, whichever is higher, and are therefore strongly suppressed.

Mean-field shifts and scattering lengths can be observed spectroscopically by driving transitions from a statistical mixture of two states to a third energy level. (While this work was in progress, use of a similar method to measure scattering lengths in fermionic ^{40}K was reported [29].) Specifically, we recorded the difference between the RF spectra for the $|2\rangle \rightarrow |3\rangle$ transition in the presence and in the absence of state $|1\rangle$ atoms. The presence of atoms in state $|1\rangle$ is then expected to shift the resonance by [30]:

$$\Delta\nu = \frac{2\hbar}{m}n_1(a_{13} - a_{12}) \qquad (1)$$

In our experimental scheme to determine the interaction energy at different magnetic fields (Fig. 2), the system was prepared by ramping up the magnetic field to 500 G with the atoms in state $|1\rangle$. Either partial or complete RF transfer to state $|2\rangle$ was then performed. The

number of atoms in state $|1\rangle$ was controlled by adjusting the speed of a frequency sweep around the $|1\rangle \rightarrow |2\rangle$ resonance. A fast, non-adiabatic sweep created a superposition of the two states, whereas a slow, adiabatic sweep prepared the sample purely in state $|2\rangle$. A wait time of 200 ms (see below) was allowed for the coherence between states $|1\rangle$ and $|2\rangle$ to decay and the system to equilibrate.

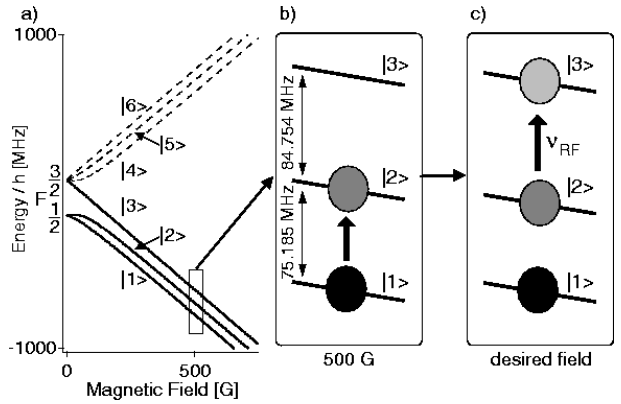

FIG. 2. Schematic of the mean-field measurement. (a) Hyperfine structure of the ground state of ^{6}Li. (b and c) Experimental scheme: (b) preparation of a mixture of atoms in states $|1\rangle$ and $|2\rangle$, and (c) RF spectroscopy of the $|2\rangle \rightarrow |3\rangle$ transition.

Typical parameters for the decohered $|1\rangle - |2\rangle$ mixture were mean-density $n_1 \sim 2.4 \times 10^{13}\,\mathrm{cm}^{-3}$ and $T \sim 0.7\,T_F$. The magnetic field was then changed to the desired value, and the transition from state $|2\rangle$ to state $|3\rangle$ was driven with 140 μs RF pulses (Fig. 2(c)). We monitored the appearance of atoms in state $|3\rangle$ and the disappearance of atoms from state $|2\rangle$, using simultaneous absorption imaging. Fig. 3(a) shows the unperturbed and perturbed resonances at $B = 480\,\mathrm{G}$. The position of the unperturbed resonance ν_{23} also determines the magnetic field to $< 0.1\,\mathrm{G}$ accuracy. Fig. 3(b) shows absorption images of atoms in state $|3\rangle$, obtained for different values of the applied radio-frequency. One can clearly see the spatial, and thus the density dependence of the mean-field shift: close to the unperturbed resonance, the low density wings of the cloud are predominantly transferred, whereas the high density central part of the cloud is transferred only at sufficient detuning. To suppress spurious effects from this spatial dependence, only a small central part of the images was used to extract the transferred atomic fraction.

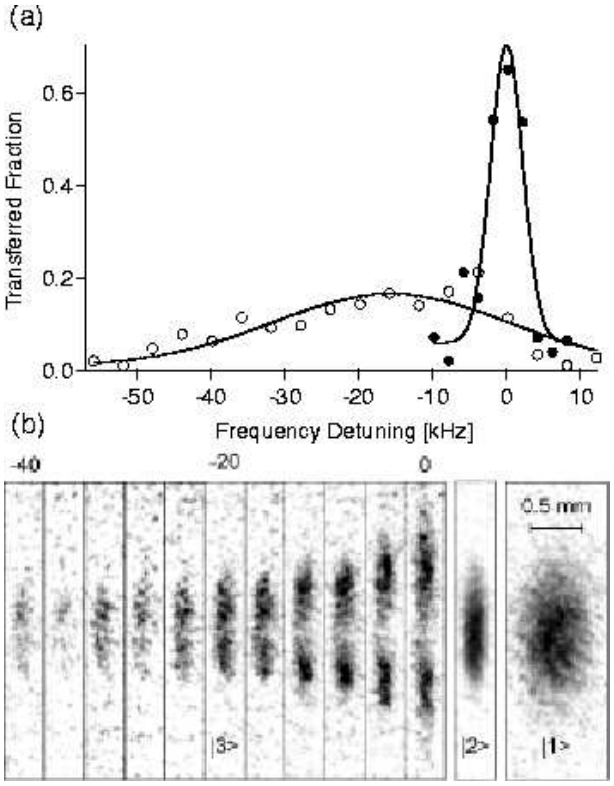

FIG. 3. Representative spectra at 480 G. (a) Fraction of atoms transferred from $|2\rangle$ to $|3\rangle$, with $|1\rangle$ atoms absent (filled circles), and present (open circles). The mean-field shift is computed from gaussian fits to the data (solid lines). (b) Spatial images of state $|3\rangle$ for the perturbed resonance. The optical trap was turned off immediately after the RF pulse and absorption images of the atoms were taken after 120 μs expansion time. The central section of $\sim$ 150 μm vertical extent was used to extract the transferred fractions in (a). (b) also shows images of states $|2\rangle$ and $|1\rangle$ for zero RF detuning. States $|3\rangle$ and $|2\rangle$ were imaged simultaneously to observe their complementary spatial structure. State $|1\rangle$ was imaged after 760 μs expansion time to record its density for normalization purposes.

To ensure that our mean-field measurements were performed on a statistical mixture, we measured the timescale for decoherence in our system. The decay of the $|1\rangle - |2\rangle$ coherence at 500 G was observed by monitoring the $|2\rangle \rightarrow |3\rangle$ transfer at the measured unperturbed resonance ν_{23}, as a function of wait time (Fig. 4). For wait times small compared to the decoherence time of the $|1\rangle - |2\rangle$ superposition, the $|2\rangle \rightarrow |3\rangle$ RF drive places each atom in an identical three-state superposition. All mean-field shifts are then absent and the resulting transfer is unchanged from the unperturbed case. For longer wait times, the $|1\rangle - |2\rangle$ superposition decoheres and mean-field interactions set in. This shifts the resonance frequency of the $|2\rangle \rightarrow |3\rangle$ transition, reducing the transferred fraction at ν_{23}. The measured decoherence time of $\sim$ 12 ms was attributed mainly to the sensitivity of ν_{12} to magnetic field variations across the cloud. These

inhomogeneities cause the relative phase of the $|1\rangle - |2\rangle$ superposition in different parts of the trap to evolve at different rates, given by the local ν_{12}. Atoms which travel along different paths within the trap therefore acquire different phases between their $|1\rangle$ and $|2\rangle$ components. Being no longer in identical states, s-wave interactions between them are allowed. The inhomogeneities scale with the applied magnetic field B while the sensitivity of the transition scales with $\partial\nu_{12}/\partial B$. We would thus expect the decoherence time to vary inversely with the product of these two quantities. Our hypothesis is supported by our observation of longer decoherence times at higher fields, where $B \times \partial\nu_{12}/\partial B$ is lower.

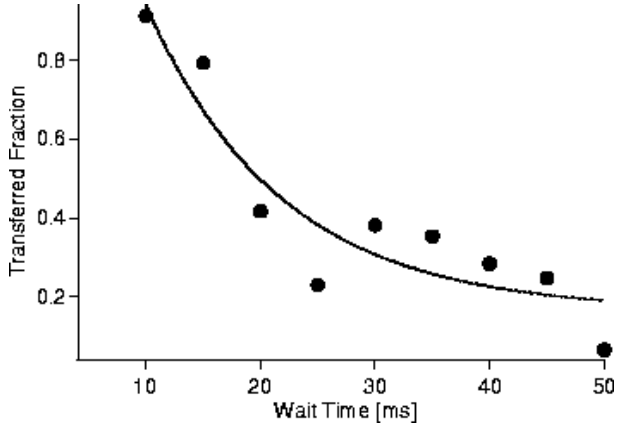

FIG. 4. Emergence of mean-field shifts due to decoherence at 500 G. Decoherence leads to a reduction of the $|2\rangle \rightarrow |3\rangle$ transfer at the unperturbed resonance ν_{23}. An exponential fit to the data (solid line) gives a time constant of 12 ms.

Fig. 5 summarizes the results of our mean-field measurements for a wide range of magnetic fields up to 750 G. For magnetic fields up to 630 G, our data can be explained fairly well using Eq. 1 with the theoretical calculations of the scattering lengths shown in Fig. 6, and an effective density of $n_1 = 2.2 \times 10^{13}\,\mathrm{cm}^{-3}$, consistent with the initial preparation of the system at 500 G. A narrow resonance of a_{12} at ~ 550 G [21,24,31] is indicated by the data, but was not fully resolved. We also see additional structure near 470 G, which is not predicted by theory and deserves further study.

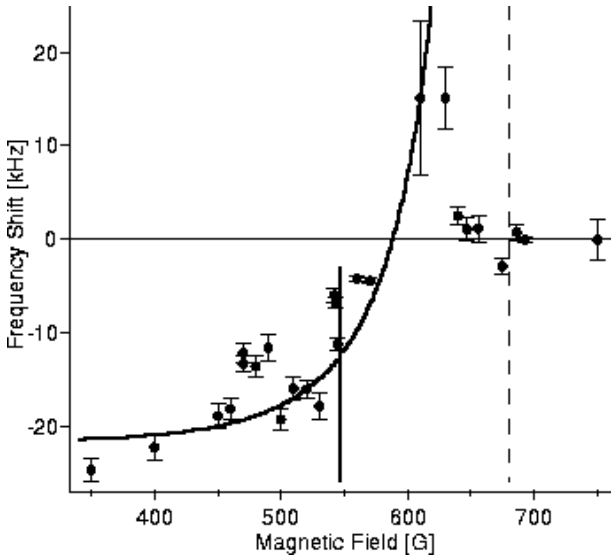

FIG. 5. Frequency shift vs. magnetic field for the $|2\rangle \rightarrow |3\rangle$ resonance due to atoms in state $|1\rangle$. The shifts are computed by monitoring the arrival fraction in state $|3\rangle$ for 140 μs RF pulses, except at 750 G. Here, because of strong inelastic losses between $|3\rangle$ and $|1\rangle$ atoms, we monitored the loss of atoms in state $|2\rangle$ after applying RF sweeps of 3 ms duration and 2 kHz width. All the data points are normalized to the same atom number in state $|1\rangle$. The fit at low fields (solid line) uses Eq. 1 with $n_1 = 2.2 \times 10^{13}\,\mathrm{cm}^{-3}$ and the theoretical calculations of the scattering lengths. The error bars reflect uncertainty in the state $|1\rangle$ atom number, and the uncertainty in the gaussian fits to the spectra. The dashed line indicates the position of the predicted a_{13} resonance.

The most important results of this paper are our observations for fields above 630 G, where the measured shifts strongly deviate from the predictions of Eq. 1. In the region between 630 G and 680 G, the two scattering lengths are expected to be large and positive, with $a_{13} \gg a_{12}$ (Fig.6). Eq. 1 would thus predict large positive mean-field shifts. In contrast, we observe very small shifts, indicating almost perfect cancellation of the two contributions. Even more surprisingly, we observe essentially no mean-field shifts between 680 G and 750 G, where the two scattering lengths are predicted to be very large in magnitude and of opposite signs, and in a simple picture should add up to a huge negative shift. These results are evidence for new phenomena in a strongly interacting system, where the scattering length becomes comparable to either the inverse wavevector of interacting particles, or the interatomic separation.

Eq. 1 is valid only for low energies and weak interactions, where the relative momentum of the two particles, $\hbar k$, satisfies $k \ll 1/|a|$. For arbitrary values of ka, the s-wave interaction between two atoms is described by replacing the scattering length a with the complex scattering amplitude:

$$f = \frac{-a}{1 + k^2 a^2}(1 - ika) \qquad (2)$$

The real part of f determines energy shifts, and hence the ground state properties of an interacting many-body system. The imaginary part determines the (inverse) lifetime for elastic scattering out of a momentum state, and hence the dynamic properties of the system such as thermalization rates. For $k|a| \to \infty$, the elastic cross-section $\sigma = 4\pi \mathrm{Im}(f)/k$ monotonically approaches the well known "unitarity limited" value of $4\pi/k^2$. On the other hand, the two particle contribution to the mean-field energy, proportional to $-\mathrm{Re}(f) = a/(1 + k^2a^2)$, peaks at $|a| = 1/k$, and then, counter-intuitively, decreases as $1/|a|$ for increasing $|a|$. It has been shown [32] that averaging $\mathrm{Re}(f)$ over a zero-temperature Fermi distribution with Fermi momentum $\hbar k_F$, limits its absolute value to $1.05/k_F$, and drastically weakens its dependence on the exact value of a in the $k_F|a| > 1$ regime. This results in a prediction for the mean-field energy which is sensitive to the sign of the scattering length, never exceeds $0.45E_F$, and remains finite for $k_F|a| \gg 1$. Hence, this approach could qualitatively explain our results in the $630 - 680$ G region, but it is in clear contradiction with negligible resonance shifts in the $680 - 750$ G region [33].

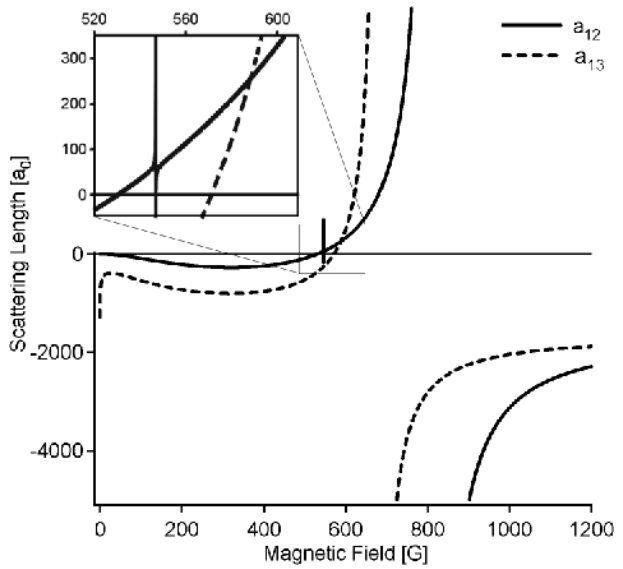

FIG. 6. s-wave scattering lengths a_{12} and a_{13} as a function of magnetic field, obtained from a highly model-independent quantum scattering calculation. The calculation makes use of the presently available ^{6}Li experimental data [39] in a coupled channel approach to deduce accumulated phases that characterize the less well-known short range parts of the ^{6}Li + ^{6}Li scattering potential [31]. a_{12} has a narrow Feshbach resonance at 550 G and a wide one at 810 G. a_{13} has a wide Feshbach resonance at 680 G.

We suggest that these discrepancies might be due to the fact that we are in the high density regime, where $n|a|^3$ approaches unity. In a degenerate Fermi gas, the interparticle spacing is comparable to the inverse Fermi wavevector, $k_F^3 = 6\pi^2 n$. Hence, the unitarity limit coincides with the breakdown of the low-density approximation ($n|a|^3 \ll 1$) and higher-order many-body effects can become important. Some recent many-body calculations [34–36] suggest that in the regime $k_F|a| \gg 1$ (or $n|a|^3 \gg 1$), the interaction energy is always negative and independent of both sign and magnitude of a. This suggests that whenever the scattering length is large, either positive or negative, the interaction energy is a universal fraction of the Fermi energy [32]. This is a possible explanation for the small line shifts that we observed for fields above 630 G, where the interactions are strong in both states.

This picture is consistent with other recent experimental observations [29,32,37,38]. Expansion energy measurements in a mixture of states $|1\rangle$ and $|2\rangle$ of ^{6}Li [38], showed a negative interaction energy at 720 G, which is on the repulsive side of the predicted Feshbach resonance. RF spectroscopy in ^{40}K [29] has also shown some saturation of the mean-field in the vicinity of a Feshbach resonance, which may reflect the unitarity limit.

In characterizing an interacting Fermi gas by RF spectroscopy, we have demonstrated absence of clock shifts in a two-level system, and introduced a three-level method for measuring mean-field shifts. For strong interactions, we have found only small line shifts which may reflect both the unitarity limit of binary collisions and many-body effects. It would be very important to distinguish between two-body and many-body effects by studying the gas over a broad range of temperatures and densities. In a very dilute and very cold gas, the weakly interacting limit could be extended to very large values of $|a|$, thus allowing for direct verification of molecular calculations. This presents experimental challenges, because cooling changes the density and the temperature together. It would also be interesting to study similar phenomena in bosonic gases, in order to distinguish to what extent the high density many-body effects depend on quantum statistics. This new insight into the physics of strongly interacting Fermi gases must be taken into account in the search for superfluidity in these systems.

[1] K. Gibble and S. Chu, Phys. Rev. Lett. **70**, 1771 (1993).
[2] C. Fertig and K. Gibble, Phys. Rev. Lett. **85**, 1622 (2000).
[3] Y. Sortais, *et al.*, Physica Scripta **T95**, 50 (2001).
[4] A. G. Martin, *et al.*, Phys. Rev. Lett. **61**, 2431 (1988).
[5] I. Bloch, T. W. Hänsch, and T. Esslinger, Phys. Rev. Lett. **82**, 3008 (1999).
[6] M. R. Matthews, *et al.*, Phys. Rev. Lett. **81**, 243 (1998).
[7] J. Stenger, *et al.*, Nature **396**, 345 (1998).
[8] M. O. Mewes, *et al.*, Phys. Rev. Lett. **78**, 582 (1997).

[9] D.M. Harber, H.J. Lewandowski, J.M. McGuirk, E.A. Cornell, Phys. Rev. A, **66**, 053616 (2002).
[10] A. Görlitz, *et al.*, Phys. Rev. Lett. **90**, 090401 (2003).
[11] T.C. Killian *et al.*, Phys. Rev. Lett. **81**, 3807 (1998).
[12] J. Stenger *et al.*, Phys. Rev. Lett. **82**, 4569 (1999).
[13] B. DeMarco and D. S. Jin, Science **285**, 1703 (1999).
[14] A. G. Truscott, *et al.*, Science **291**, 2570 (2001).
[15] F. Schreck, *et al.*, Phys. Rev. Lett. **87**, 080403 (2001).
[16] S. R. Granade, M. E. Gehm, K. M. O'Hara, and J. E. Thomas, Phys. Rev. Lett. **88**, 120405 (2002).
[17] Z. Hadzibabic, *et al.*, Phys. Rev. Lett. **88**, 160401 (2002).
[18] G. Roati, F. Riboli, G. Modugno, and M. Inguscio, Phys. Rev. Lett. **88**, 160401 (2002).
[19] M. Houbiers and H. T. C. Stoof, Phys. Rev. A **59**, 1556 (1999).
[20] M. Holland, S. J. J. M. F. Kokkelmans, M. L. Chiofalo, and R. Walser, Phys. Rev. Lett. **87**, 120406 (2001).
[21] K. Dieckmann *et al.*, Phys. Rev. Lett. **89**, 203201 (2002).
[22] Z. Hadzibabic *et al.*, arXiv:cond-mat/0306050 (2003).
[23] M. Houbiers, H. T. C. Stoof, W. I. McAlexander, and R. G. Hulet, Phys. Rev. A **57**, R1497 (1998).
[24] K. M. O'Hara, *et al.*, Phys. Rev. A **66**, 041401 (2002).
[25] The transfer efficiency is limited by finite optical trap depth and residual heating during the transfer.
[26] K. Gibble and B. J. Verhaar, Phys. Rev. A **52**, 3370 (1995).
[27] For our modest degeneracy, we can use a gaussian approximation for the density distribution. The mean density is then lower than the peak density by a factor of $2\sqrt{2}$.
[28] Our estimate uses the direct mean-field measurement of Bourdel *et. al.* [38] scaled to our parameters .
[29] C.A. Regal, D.S. Jin, Phys. Rev. Lett. **90**, 230404 (2003).
[30] Note that due to fermionic antisymmetry, there is no clock shift from interactions between atoms in states $|2\rangle$ and $|3\rangle$. Mean field shifts only arise during a decoherence time (see later in the text), but are negligible if the population of atoms in state $|3\rangle$ is small.
[31] E. G. M. van Kempen *et al.*, in preparation (2003).
[32] M.E. Gehm, S.L. Hemmer, S.R. Granade, K.M. O'Hara, J.E. Thomas, Phys. Rev. A, **68**, 011401(R) (2003).
[33] We note that for fields above 630 G, number losses generally reduced n_1, and all the shifts in this region were scaled up by a factor of $1.1 - 2.7$, but still remained negligible.
[34] J. V. Steele, arXiv:nucl-th/0010066 (2000).
[35] H. Heiselberg, Phys. Rev. A **63**, 043606 (2001).
[36] R. Combescot, arXiv:cond-mat/0302209 (2003).
[37] K.M. O'Hara, S.L. Hemmer, M.E. Gehm, S.R. Granade, J. E. Thomas, Science, **298**, 2179 (2002).
[38] T. Bourdel, *et al.*, arXiv:cond-mat/0303079 (2003).
[39] This includes the recent measurement of 800 ± 40 G for the resonance in a_{12} [38].
[40] The work at MIT was supported by the NSF, ONR, ARO, and NASA. The work at Eindhoven was supported by FOM (NWO).